JOURNAL OF CATALYSIS **168,** 16–25 (1997)
ARTICLE NO. CA971573

Reducibility of Cobalt Species in Silica-Supported Fischer–Tropsch Catalysts

A. Yu. Khodakov,* J. Lynch,*,[1] D. Bazin,† B. Rebours,* N. Zanier,* B. Moisson,* and P. Chaumette*

*Institut Français du Pétrole, B. P. 311,92506 Rueil-Malmaison Cedex, France; †Laboratoire pour l'Utilisation de Rayonnement Electromagnétique, Université Paris-Sud, 91405 Orsay, France

Received July 12, 1996; revised October 24, 1996; accepted December 9, 1996

Reducibility of Co species in silica supported Fischer–Tropsch catalysts was studied using *in situ* XRD, *in situ* EXAFS, and FTIR spectroscopy with carbon monoxide as a molecular probe. Crystalline Co phases in the oxidised catalysts were characterised using XRD. In the oxidised samples with a large concentration of amorphous phase, EXAFS showed the presence of small oxide clusters including several Co atoms. It was found (*in situ* XRD, EXAFS) that calcination of oxidised Co catalysts under inert atmosphere resulted in a selective transformation of Co_3O_4 to CoO at 623–673 K. FTIR spectroscopy with CO as a molecular probe revealed the presence of different sites associated with Co after the reduction of the catalysts with hydrogen at 723 K: Co metal sites ($\nu_{CO} = 2025\ cm^{-1}$), Co^{2+} ions in the crystalline phase of CoO ($\nu_{CO} = 2143\ cm^{-1}$), and Co^{n+} species in the amorphous phase ($\nu_{CO} = 2181\ cm^{-1}$). The results (XRD, EXAFS, FTIR) showed that the hydrogen reduction properties of particles of cobalt oxide on silica depended on the size of the Co_3O_4 crystallites. The ease of reduction to metal species decreased from larger (200–700 Å) to smaller (60 Å) particles.

INTRODUCTION

Cobalt containing catalysts are known to be effective in the Fischer Tropsch synthesis (1–4). The activity and selectivity of Co supported catalysts towards different hydrocarbons are strongly dependent on the preparation conditions such as impregnation or co-precipitation followed by calcination and reduction with hydrogen or other gaseous reducing agents. The activity of Co catalysts in the Fischer–Tropsch synthesis is usually attributed to the active sites located on the surface of supported cobalt metal particles formed after the reduction (5).

A number of investigations has been focused so far on the nature of cobalt species on various supports: alumina (6–13), silica (7, 9, 14–19), titania (7, 20, 21), magnesia (7, 20), carbon (20, 22), and ZSM-5 zeolite (23, 24). Various techniques have been employed: X-ray diffraction (XRD), temperature-programmed reduction (TPR), X-ray photoelectron spectroscopy (XPS), Fourier transform infrared spectroscopy (FTIR), and extended X-ray absorption fine structure (EXAFS), etc. X-ray diffraction which permits the size and concentration of oxide and metal crystallites to be measured is one of the most common. Different Co species were reported to be found in the oxide precursors of Fischer–Tropsch catalysts using XRD: (1) Co_3O_4 oxide crystalline phase; (2) CoO crystalline phase; (3) Co^{3+} ions or/and Co^{2+} located in Al^{3+} or Si^{4+} oxidic crystallites or in well dispersed surface species; (4) $CoAlO_4$ or Co_2SiO_4 crystalline or/and amorphous phase.

FTIR has been used to identify the nature of active sites in Co_3O_4, Co/Al_2O_3 modified with different promoters and Co/SiO_2 catalysts as well (12, 13, 25–27). Reduced Co species in these catalysts were characterised by the bands of adsorbed CO at 2000–2070 cm^{-1}, the oxidised species showing the bands of adsorbed CO at 2160–2180 cm^{-1}. Modification of Co catalysts with promoters results in modification of the electronic properties of oxidised and reduced forms and in the appearance of additional bands in the spectra of adsorbed CO.

EXAFS is nowadays one of the most powerful methods of local order characterisation in highly dispersed metal catalysts (28, 29). This method is especially useful for investigation of the environment of amorphous phases and small metal particles which are very difficult to study by other techniques. In many cases information can be gathered (*in situ*) during the processes of preparation, when the catalyst is inaccessible to traditional surface analysis.

As was shown earlier in the literature (5–19), the reducibility of Co species in oxide supported catalysts depends on the nature of the support and the Co distribution between different supported phases (crystalline Co_3O_4, "cobalt silicate," etc.). However, little information is actually available on the structure of amorphous species in Co/silica catalysts and on the reducibility of supported Co_3O_4 crystallites with different particle sizes.

In this paper we study the nature and reducibility of Co species in the oxidised precursors of silica supported

[1] Address for correspondence: Dr. John Lynch, Physics and Analysis, Institut Français du Pétrole, Boite Postale 311, 92506 Rueil-Malmaison Cedex, France. Fax: +33 1 47 52 70 57. E-mail: john.lynch@ifp.fr.

0021-9517/97 $25.00

catalysts using *in situ* X-ray diffraction, *in situ* EXAFS, and FTIR spectroscopy with CO as a molecular probe. *In situ* X-ray diffraction allowed the changes in crystallographic order of cobalt species during their treatment with hydrogen or under inert atmosphere to be followed. EXAFS was used to investigate the structural environment of Co atoms in oxidised samples and also *in situ* during reduction with hydrogen and under inert atmosphere. FTIR spectroscopy was employed to study the nature and number of surface sites generated after the reduction of the catalysts.

METHODS

Catalysts

Five Co-supported catalysts (cobalt loading ≈24 wt%), as well as pure silica were studied (Table 1). The samples were prepared by the hydrolysis of tetraethyl silicate in the presence of cobalt nitrate. First, the tetraethyl silicate, an alcohol, nitric acid, and cobalt nitrate were mixed in a glass flask (tetraethyl silicate/H_2O/ROH/HNO_3 = 1/10/3/0.5). The alcohols used for the catalyst preparation are presented in Table 1. The viscosity of the reaction mixture increased progressively up to the gel formation. The duration of such treatment was 30 min. The time of gel maturation was fixed at 150 min. The samples were then dried for 24–48 h at 373 K and calcined for 3 h at 873 K. The surface of the samples was measured by low temperature adsorption of nitrogen using the BET equation. The samples after calcination were also characterised by XRD (Cu(K_α)).

XRD Measurements

In situ XRD measurements were carried out using Cu(K_α) radiation on a Siemens diffractometer equipped with an Anton Paar KG reactor chamber. The reactor chamber mounted on a goniometer permitted studies of catalysts under *in situ* conditions. The powdered samples (0.200 g each) were placed on a clean ceramic slide and pressed by hand. During *in situ* X-ray diffraction reaction gases passed through the samples at temperatures from ambient to 823 K. The gases used for experiments (H_2 or N_2—Air Liquide) had a purity of 99.995%. Gas pressure was approximately 1 bar. Prior to diffraction measurements the samples were heated under nitrogen or hydrogen for 30 min at the chosen temperature.

TABLE 1

Co-Supported Silica Catalysts

Sample	wt% Co	Alcohols used for synthesis	$D_{Co_3O_4}$, Å	%Co_3O_4 crystal, XRD	S_{BET}, m^2/g
1FTCAT	24.78	Ethanol/ formamide = 1 : 1	60	56	513
2FTCAT	26.85	Ethanol	110	64	341
3FTCAT	25.65	*n*-Hexanol	150	40	245
4FTCAT	23.35	Methanol	200	73	270
5FTCAT	23.48	*n*-Butanol	700	12	360

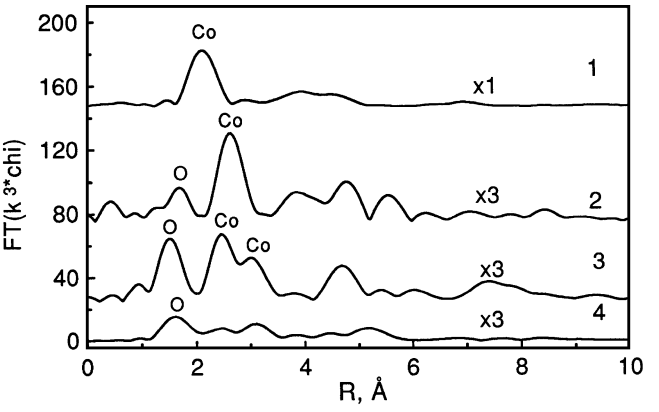

FIG. 1. Fourier transform moduli of EXAFS for Co foil (1), CoO (2), (3) Co_3O_4, and (4) orthorhombic cobalt silicate (room temperature).

EXAFS

The experiments were carried out in the Laboratoire pour l'Utilisation de Rayonnement Electromagnétique (Orsay) at the EXAFS4 beam line using synchrotron radiation from the DCI storage ring running at 1.85 GeV with an average current of 250 mA. The EXAFS data were taken in the transmission mode through a double crystal monochromator (Si(111)) using two ion chambers as detectors. The EXAFS unit equipped with a heater, a water cooling system, thermocouples, and a system of gas circulation allows *in situ* treatment of samples at temperatures 298–773 K. Total reduction time was 85 min. The apparatus is identical to that designed by Lytle (28, 30). The 1FTCAT and 4FTCAT samples were reduced *in situ* using a temperature programme (298–723 K, 5°/min). The time of measuring an X-ray absorption spectrum (7550–8400 eV) was about 40 min.

The Co K-edge extended X-ray absorption fine structure region of the spectra for Co/silica catalysts was analysed using the standard data analysis procedure (SIMPLEX software package (31)). The EXAFS spectrum was first transformed from k space (k^3, Hanning windows 2.8, 4.2, 10.4, 12 $Å^{-1}$) to r space to obtain the radial distribution function (RDF). The EXAFS spectrum for one or several coordination shells was isolated by inverse Fourier transform of the RDF over the appropriate region and fitted using the single scattering EXAFS equation.

The moduli of the Fourier transforms of EXAFS and structural data for Co_3O_4, CoO, Co foil, and orthorombic cobalt silicate are shown in Fig. 1 and in Table 2,

TABLE 2

Interatomic Distances (R) and Coordination Numbers (N) for the Co Model Compounds

Sample	R, Å	N	Sample	R, Å	N
Co metal			CoO		
Co–Co	2.51	12	Co–O	2.13	6
Co–Co	3.57	6	Co–Co	3.02	12
Co–Co	4.36	24	Co–O	3.69	8
Co–Co	5.02	12	Co–Co	4.27	6
Co–Co	5.62	24			
Co_3O_4			Co_2SiO_4		
Co–O	1.89	4	Co–O	2.08	3.5
Co–O	1.98	1.33	Co–O	2.20	2.5
Co–Co	2.85	4	Co–Si	2.73	1
Co–Co	3.35	8	Co–Si	2.80	0.5
			Co–Co	3.00	1
			Co–Co	3.22	2

respectively. As can be seen from Fig. 1, in the Fourier transform modulus of Co_3O_4 several peaks attributed to different Co coordination shells can be observed. First, we separated the peaks attributed to CoO coordination shells and to CoCo coordination shells (see Table 2 and Fig. 1), the corresponding inverse Fourier transforms were made in the ranges of 1.18–2.02 Å and 2.02–3.57 Å.

Co_3O_4 has a spinel type structure, where Co^{2+} cations have a tetrahedral coordination and Co^{3+} are octahedrally coordinated with oxygen atoms. These two Co–O coordination shells are usually not separated in the Fourier transform moduli of Co_3O_4 and the Co supported samples (32). For this reason, we fitted them with single shell parameters assuming that the shell contains disorder, i.e., a larger value of the Debye–Waller factor as compared with that for a single shell.

The second and third Co coordination shells in Co_3O_4 consists of Co atoms (N = 4, R = 2.85 Å and N = 8, R = 3.35 Å). As can be seen from Fig. 1, the peaks in the Fourier transform attributed to CoCo second and third coordination shells are overlapped. Thus, the inverse Fourier transform in the region of 2.02–3.57 Å was fitted using the parameters for two CoCo coordination shells at R ≈ 2.85 Å and R ≈ 3.35 Å.

The phases and amplitudes for CoO and CoCo coordinations were calculated *ab initio* using the FEFF5 code (33). Three cluster models were employed. An octahedron CoO_6 with a CoO distance of 1.89 Å was adopted for evaluation of the phase and amplitude functions for the CoO shell. The phases and amplitudes for the first ($d_{CoCo} = 2.85$ Å) and the second ($d_{CoCo} = 3.35$ Å) CoCo coordination shells were calculated using two different cluster models. The clusters used contained only the Co atoms of the corresponding coordination shells. The atoms in the clusters were located relative to the central atom at the same positions as in the crystal of Co_3O_4. In the second cluster employed to calculate the phase and amplitude for CoCo distance of 3.35 Å, the central Co atom was placed in the crystallographic site corresponding to the Co^{3+} ions in the Co_3O_4 spinel structure.

As can be seen from Table 3, the coordination parameters for Co_3O_4 evaluated using the theoretical phases and amplitudes calculated using FEFF, are very close to those known from the literature. The residuals of the fits which were estimated using the values of mean squared deviations (Δ^2) are also shown in Table 3.

The uncertainty in the coordination numbers (ΔN) evaluated from EXAFS data is usually less than 20% in the most desirable case, for which the least-squares fitting involves only a single coordination shell which is well resolved from its neighbouring shells. ΔN increases when the calculation involves more than one shell and is extended to the coordination shells beyond the nearest shell. Therefore, in our case, the uncertainty in N may be larger than 20%. However, it should be noted that no attempt was made in this work to determine quantitatively the distribution of different phases and the Co particle sizes using the results of EXAFS analysis.

TABLE 3

Results of EXAFS Fitting for Calcined Co/Silica Catalysts

	N CoO	R_{CoO} (Å)	σ (Å)	Δ^2, 10^{-3}	N CoCo	R_{CoCo} (Å)	σ (Å)	N CoCo	R_{CoCo} (Å)	σ (Å)	Δ^2, 10^{-2}
Co_3O_4	5.3	1.92	0.02	1.2	3.8	2.83	0.07	8.4	3.34	0.08	3.1
1FTCAT	4.0	1.91	0.03	4.2	3.4	2.84	0.08	4.5	3.37	0.09	6.9
2FTCAT	5.3	1.92	0.03	6.3	4.0	2.84	0.08	7.5	3.35	0.10	5.7
3FTCAT	4.0	1.94	0.07	7.6	3.6	2.86	0.11	1.5	3.38	0.09	7.0
4FTCAT	4.9	1.92	0.02	5.1	4.3	2.85	0.08	7.5	3.37	0.07	6.3
5FTCAT	4.3	1.93	0.05	2.2	2.0	2.83	0.08	3.4	3.35	0.09	5.8
Inverse Fourier transform region		1.18–2.02 Å						2.02–3.57 Å			

Note. N and R are a calculated coordination number and an interatomic distance, σ is a Debye–Waller factor, Δ^2 is a fit residual.

FTIR Measurements

The FTIR spectra were measured using a DIGILAB FTS 80 spectrophotometer in a quartz cell with KBr windows which allows the samples to be treated under vacuum or under various gases at higher temperatures. Before carbon monoxide adsorption the samples (∼16–17 mg) were heated over night at 493 K under vacuum, then they were exposed to hydrogen ($p = 250$ mbar) and treated consequently under hydrogen at 553 K and 623 K for 10 min and at 723 K for 40 min. The rate of temperature increase in XRD and FTIR experiments was 5°/min. Carbon monoxide was adsorbed on the catalysts at room temperature ($p_{CO} =$ 0–35 mbar).

RESULTS

1. Cobalt Species in the Oxidised Catalysts

The XRD patterns of the oxidised samples are presented in Fig. 2. After calcination only a Co_3O_4 crystalline phase can be observed by XRD. Co distribution between amorphous and crystalline phases and the sizes of Co_3O_4 crystallites were estimated using the intensities and widths (Scherrer equation (34)) of XRD peaks ($2\theta = 59.345°$ (511) Co_3O_4). A mechanical mixture of crystalline Co_3O_4 and silica (24 wt% Co) was used as a reference to evaluate the concentration of the Co_3O_4 crystalline phase in the samples from XRD. The average particle size and the percentage of Co in the Co_3O_4 crystalline phase in the samples estimated from XRD are shown in Table 1.

As can be seen from the comparison of the moduli of Fourier transforms of EXAFS for Co_3O_4 and the oxidised catalysts (Figs. 1 and 3), after calcination the Co atoms in the Co/silica catalysts have an environment rather similar to that in Co_3O_4: in the first coordination sphere they are likely to be surrounded by oxygen atoms, in the second and third sphere by Co atoms. In the silica supported catalysts,

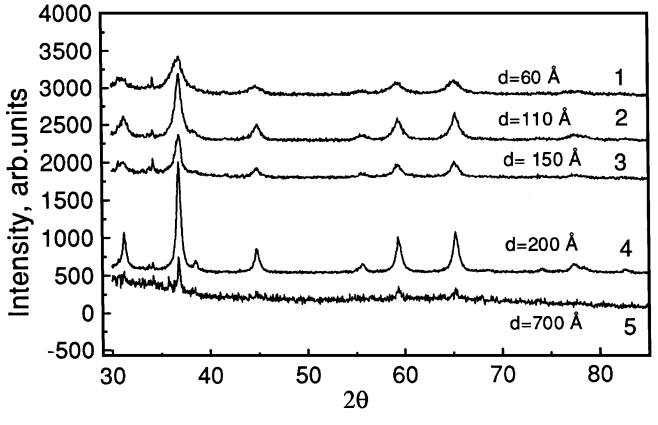

FIG. 2. XRD patterns of the calcined Co/silica catalysts measured at room temperature (1, 1FTCAT; 2, 2FTCAT; 3, 3FTCAT; 4, 4FTCAT; 5, 5FTCAT).

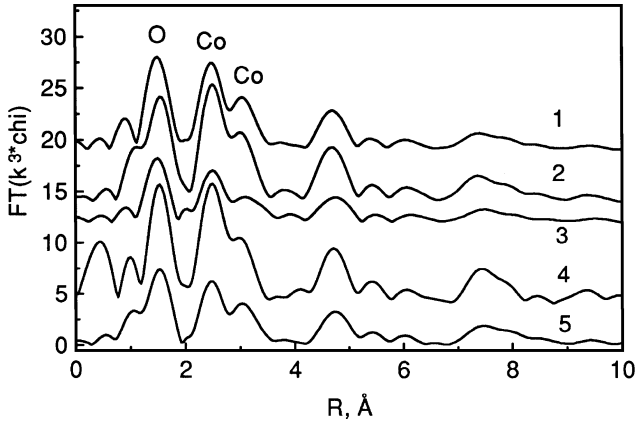

FIG. 3. Fourier transform moduli of EXAFS for 1, 1FTCAT; 2, 2FTCAT; 3, 3FTCAT; 4, 4FTCAT; 5, 5FTCAT. The samples were calcined under air at 873 K.

however the presence of silicon atoms in the coordination sphere of Co cannot be excluded.

The EXAFS data were analysed in the same manner as for Co_3O_4. The phases and amplitudes for CoO and CoCo distances were calculated *ab initio* (FEFF5 code) using the cluster models described above. The inverse Fourier transform was performed over the 1.18–2.02 and 2.02–3.57 Å region.

As can be seen from Table 3, the coordination number and distances for the Co–O coordination shell are very close to that in Co_3O_4; however, the σ is higher for the more amorphous 3FTCAT and 5FTCAT samples (see Table 1) than for the 2FTCAT and 4FTCAT crystalline catalysts. The average interatomic distances for the Co–O coordination shell were found to be nearly the same in all the samples. The Co–O coordination number for the catalysts was always between 4 and 6, because the Co ions assemble as many oxygen atoms around them as possible.

The second and third Co coordination sphere of the Fischer–Tropsch catalysts can contain Co or/and Si atoms. Coordination of Co with Si atoms in the second coordination shell can be expected in particular for the 3FTCAT and 5FTCAT samples with a large concentration of amorphous phase which may contain isolated Co^{n+} atoms incorporated in the silica matrix. However, fitting of the filtered EXAFS (2.02–3.57 Å) using theoretical amplitudes and phases for Co–Si and Co–Co coordination spheres ($R_{CoSi} = R_{CoCo} = 3$ Å) calculated using the FEFF5 code showed that the contribution to EXAFS arising from the Co–Si shell would be very small. Very low intensity of EXAFS from a CoSi coordination relative to that of a Co–Co coordination suggests that even if Si atoms are situated at a distance of approximately 3 Å from the central Co atom, they are very difficult to detect relative to Co atoms.

The fitting of the inverse Fourier transform for the second and third coordination shells showed (Table 3) very similar Co–Co coordination numbers ($N_{CoCo} \sim 4$–4.5 for the

second shell and $N_{CoCo} = 7–8$ for the third one) for the 2FTCAT and 4FTCAT samples which contain a large concentration of Co_3O_4 crystalline phase, whereas the CoCo coordination number for the amorphous 5FTCAT was remarkably lower ($N_{CoCo} \sim 2$ for the second shell). However, the uncertainty in determination of CoCo coordination number from EXAFS makes it difficult to estimate the concentration of amorphous and crystalline phase in the samples quantitatively. Examples of the fitting for the 4FTCAT and 5FTCAT samples are shown in Figs. 4a and b.

The results obtained show that, both in the 2FTCAT, 4FTCAT catalysts with a large concentration of Co_3O_4 crystallites and in the 3FTCAT and 5FTCAT catalysts which contain more amorphous Co species, Co atoms on average have Co atoms in the second and third coordination sphere. The comparison of Fourier transform moduli of the 5FTCAT sample and Co_3O_4 (Figs. 1 and 3) shows that in the amorphous oxide phase Co atoms are likely to have the same type of structural environment as in Co_3O_4 even at longer distances (up to 8 Å). As seen also from Figs. 1 and 3, the Fourier transform modulus of 5FTCAT containing 88% of cobalt in the XRD amorphous phase is quite different from the modulus of orthorombic silicate, for example the average Co–O distance in silicate is longer (~2.08–2.20 Å) than in the 5FTCAT (~1.93 Å).

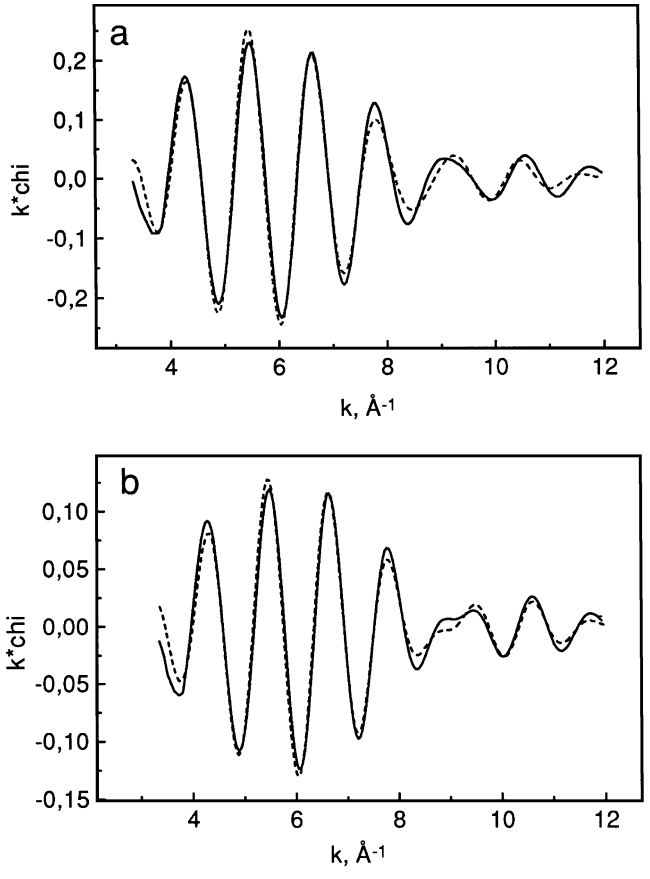

FIG. 4. Results of EXAFS fitting for the 4FTCAT (a) and 5FTCAT (b) samples—inverse Fourier transform range –2.02–3.57 Å (———, experimental curve, – - -, calculated curve).

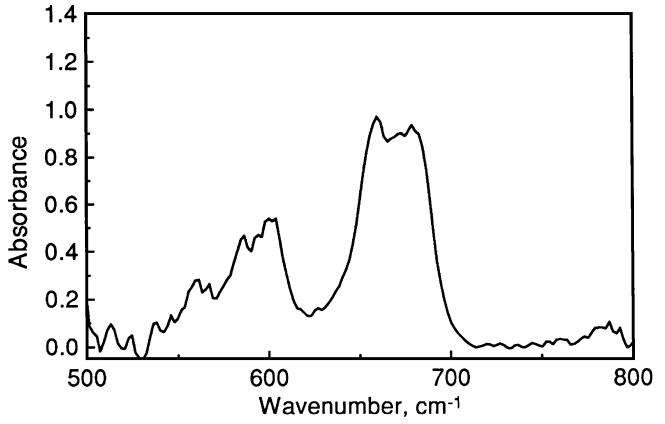

FIG. 5. FTIR spectra of the 4FTCAT sample in the region of the Co_3O_4 structural bands measured at 493 K before its decomposition to CoO.

Co_3O_4 crystals are characterised in the FTIR spectra by the broad bands (35) at 670 and 550–600 cm^{-1} (Fig. 5). Treatment of the samples at 553 K under hydrogen results in a disappearance of these bands that is related, as we shall see later, to the reduction of the Co_3O_4 phase to CoO. Crystalline CoO does not have any intense bands in the vibrational spectra and was difficult to identify using FTIR.

2. *Decomposition of Co_3O_4 Supported by Silica under Inert Atmosphere*

The XRD patterns of the 4FTCAT sample measured at different temperatures under nitrogen are shown in Fig. 6. Heating of the sample at 623–673 K results in decomposition of the Co_3O_4 crystalline phase and its selective transformation to the CoO phase. CoO was the only crystalline phase observed after calcination under nitrogen at

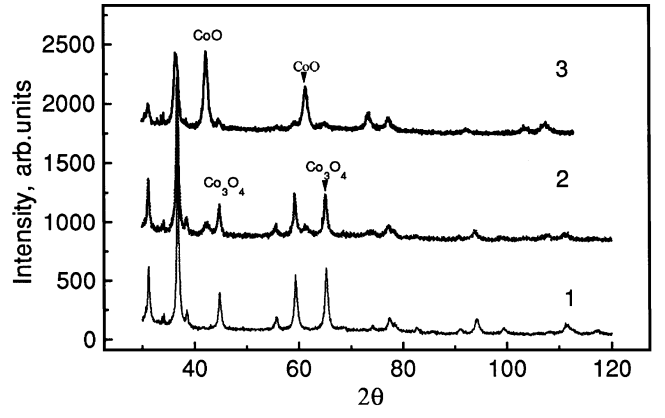

FIG. 6. XRD patterns of the 4FTCAT sample measured under nitrogen at different temperatures (1, room temperature; 2, 623 K; 3, 673 K).

723 K. Treatment of the samples at higher temperature (773–873 K) did not cause any considerable changes in the XRD patterns of the samples.

Decomposition of Co_3O_4 on heating under inert atmosphere was also observed on other Co/SiO_2 samples. At the same time, no decomposition was observed on heating bulk crystalline Co_3O_4 under nitrogen up to 823 K. Thus it can be suggested that the chemical and physical properties and especially the reducibility of relatively small Co_3O_4 oxide crystallites (d = 60–200 Å) are different from those of the bulk oxide.

The effect of heating under inert atmosphere on the oxidation state of Co was also followed by EXAFS. The moduli of the 4FTCAT sample heated under nitrogen at 723 K and at room temperature are shown in Fig. 7. Analysis of the data shows that such treatment results in almost complete transformation of Co_3O_4 crystalline phase to CoO that is in good agreement with the XRD data.

3. *Reduction under Hydrogen*

In Figs. 8a, b the XRD patterns of the 1FTCAT and 4FTCAT samples measured *in situ* during reduction under hydrogen are shown. Compared to treatment under inert atmosphere, treatment under hydrogen leads to much easier reduction of the Co_3O_4 crystalline phase to CoO and also to consecutive reduction of the CoO phase to metal. The reduction to CoO proceeds at approximately 473 K, as compared to the decomposition under nitrogen which occurred at 623–673 K (Fig. 6), the consecutive reduction of CoO to Co metal starts from 523–573 K.

The XRD patterns of the samples reduced at 723 K under hydrogen are shown in Fig. 9. The reduction results in the formation of two Co metal phases: cubic and hexagonal with a predominance of the cubic form. As seen from Fig. 8, for all the samples treatment with hydrogen resulted in complete reduction of the Co_3O_4 to CoO, whereas the extent of the reduction to metal phases varied depending on the samples. The highest relative concentrations of reduced cobalt were observed on the samples with larger particles (4FTCAT and 5FTCAT). For the samples with relatively small particles of Co_3O_4 (1FTCAT) a considerable

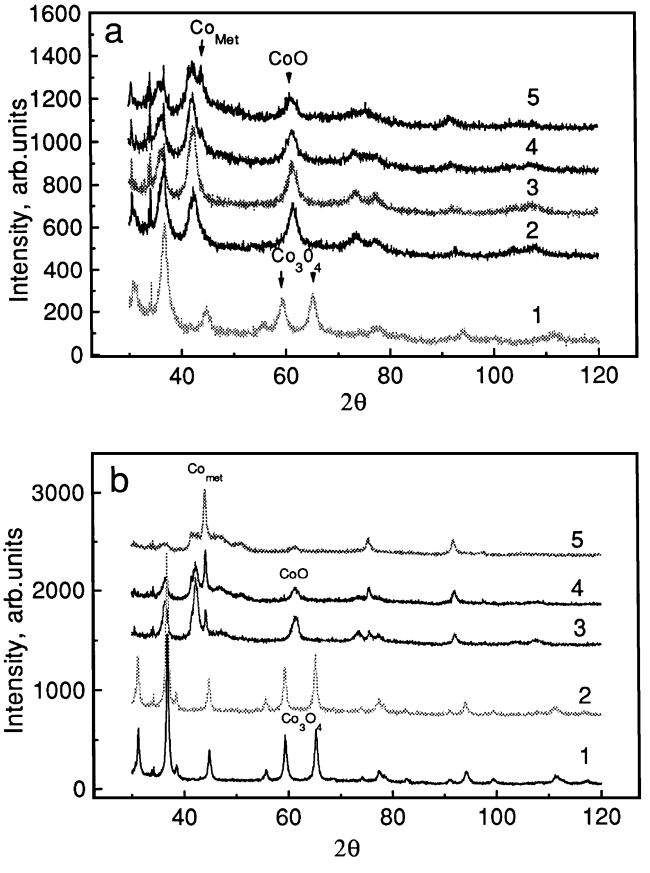

FIG. 8. XRD patterns of the 1FTCAT (a: 1, room temperature; 2, 523 K; 3, 623 K; 4, 723 K; 5, 823 K) and the 4FTCAT (b: 1, room temperature; 2, 473 K; 3, 573 K; 4, 623 K; 5, 723 K). Samples measured at different temperatures under hydrogen.

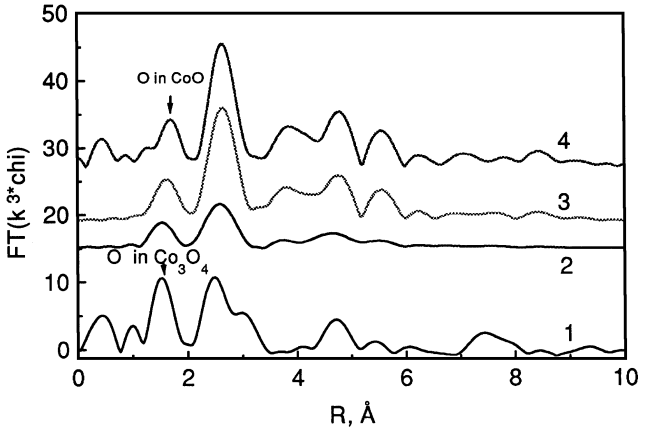

FIG. 7. Fourier transform moduli of EXAFS for the 4FTCAT catalyst treated with nitrogen at different temperatures (1, 293 K; 2, 723 K; 3, at 293 K after treatment under nitrogen at 723 K; 4, CoO at 293 K).

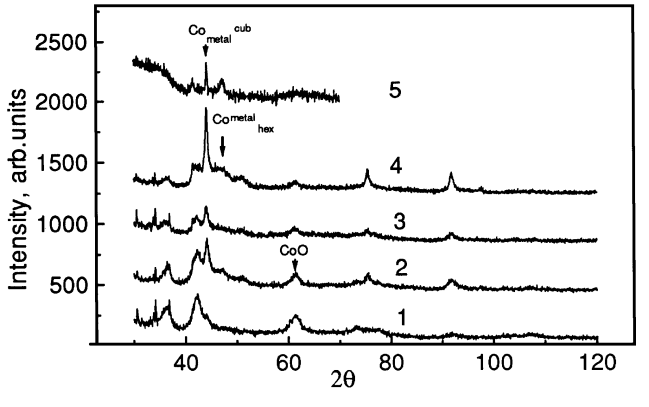

FIG. 9. XRD patterns of the Co/silica samples reduced with hydrogen at 723 K (1, 1FTCAT; 2, 2FTCAT; 3, 3FTCAT; 4, 4FTCAT; 5, 5FTCAT).

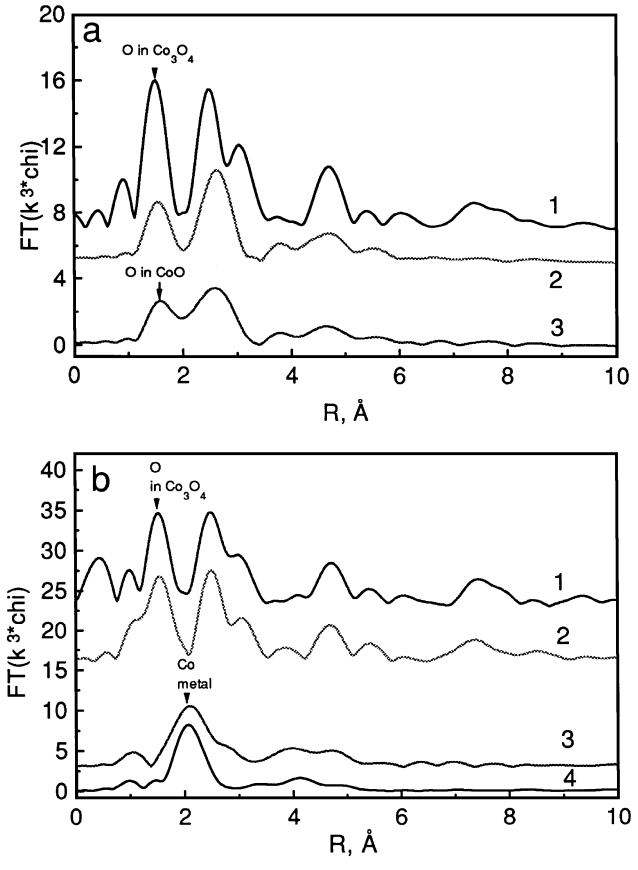

FIG. 10. Moduli of Fourier transform of EXAFS for the 1FTCAT (a: 1, 293 K; 2, 623 K; 3, 773 K) and the 4FTCAT (b: 1, 293 K; 2, 423 K; 3, 623 K; 4, 773 K). Catalysts treated with hydrogen at different temperatures.

concentration of the CoO crystallites was still found even after treatment with hydrogen at 723–773 K for several hours.

The moduli of Fourier transforms of EXAFS for the 1FTCAT and 4FTCAT samples during treatment *in situ* with hydrogen are shown in Figs. 10a, b. The Co coordination after treatment of the samples at 423 K is nearly the same as in the starting materials, whereas the treatment at 623 K leads to the reduction of Co species. After treatment with hydrogen at 773 K the Co coordination shell in the 4FTCAT sample was found to be nearly the same as in the bulk Co corresponding to practically complete reduction of the oxide phase to metal, whereas in the 1FTCAT samples with smaller Co crystalline particles treatment with hydrogen resulted only in a formation of CoO species. Comparison of the Fourier transform moduli demonstrates a rather high extent of reduction of Co oxides to metal in the 4FTCAT sample already at 623 K and a very low concentration of metal species in the 1FTCAT sample even after treatment with H_2 at 773 K.

The reduction of Co_3O_4 crystalline phase in the Fischer–Tropsch catalysts was also followed by FTIR. The surface sites in the catalysts after reduction at different temperatures were identified by using FTIR with adsorbed CO. The spectra of CO adsorbed on the 4FTCAT sample reduced in the temperature region 493–723 K followed by evacuation at the same temperature are shown in Fig. 11. As can be seen, after treatment with hydrogen at 493 K only a small concentration of oxidised Co^{n+} ($n = 2, 3$) species, which can be identified (25, 26) by the band at 2181 cm^{-1}, is observed. Treatment of the catalysts at 553 K with hydrogen results in an appearance of two new bands at 2143 cm^{-1} and 2025 cm^{-1} which correspond to CO complexes with the reduced Co species. In accordance with the data of Heal (26), Moon (27), and Kazansky (12, 13), the band at 2025 cm^{-1} can be attributed to CO adsorbed on Co metal sites. As seen from the spectra (Fig. 11) these bands are the most intense after treatment with hydrogen at 623 K. Further reduction of the 4FTCAT sample did not lead to an increase in the intensity of the band at 2025 cm^{-1}, which suggests that the number of metal sites in the 4FTCAT samples is practically the same after treatment at 723 K as at 623 K. A decrease in the pressure of CO adsorbed on the samples at room temperature leads to almost complete disappearance of the bands at 2181 cm^{-1} and 2143 cm^{-1}, the maximum of the band at 2025 cm^{-1} being shifted to lower frequencies.

The FTIR spectra of the samples after reduction at 723 K with adsorbed CO are shown in Fig. 12. Adsorption of CO on the reduced Co catalysts leads to the appearance of peaks in the region of 1800–2200 cm^{-1} which can be attributed to CO interaction with different surface sites.

The band at 2181 cm^{-1} is likely due to hardly reducible Co oxidised species. This band was the most intense for the 5FTCAT sample, where the concentration of crystalline Co_3O_4 is rather low and most of Co is in the amorphous phase. The assignment of the band at 2181 cm^{-1} to the complexes of CO with oxidised Co species is supported by the fact that this band was also observed in the FTIR spectra after

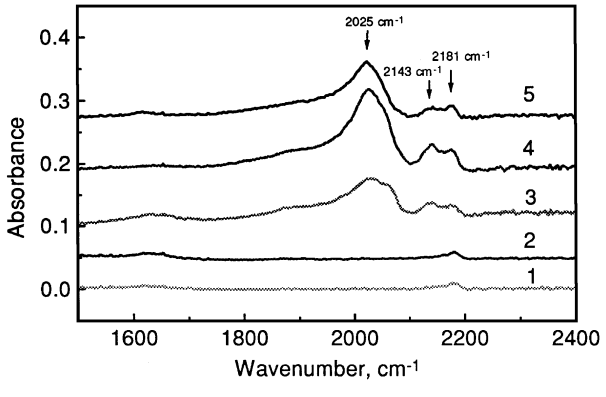

FIG. 11. FTIR spectra of CO ($p_{CO} = 35$ mbar) adsorbed on the 4FTCAT sample reduced at different temperatures (1, T = 493 K after heating under vacuum prior to the reduction; 2, 493 K; 3, 553 K; 4, 623 K; 5, 723 K).

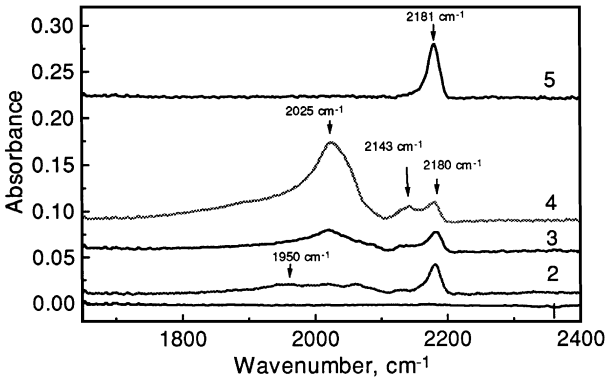

FIG. 12. FTIR spectra of CO ($p_{CO} = 35$ mbar) adsorbed on the samples reduced at 723 K (1, silica; 2, 1FTCAT; 3, 3FTCAT; 4, 4FTCAT; 5, 5FTCAT).

calcination of the samples under vacuum without hydrogen treatment.

The band at 2143 cm^{-1} seems to be attributable to Co^{2+} ions located in the CoO phase which is an intermediate species during the reduction of Co_3O_4 to Co metal. There are several arguments in favour of this assignment: (i) this band can be observed only in the spectra of the partially reduced samples; (ii) its intensity is correlated with the intensity of XRD peaks attributed to the CoO crystalline phase; (iii) the frequency of this band (very small shift relative to ν_{CO} in gas phase) gives evidence to attribute this band to the CO complexes with partially reduced cations (oxidation state—between Co^{3+} and Co^0).

Low frequency bands at 1900–2000 cm^{-1} can be assigned to CO adsorbed on metal particles. The position of these bands was found to vary as a function of CO coverage of Co/silica samples due to the well-known effect of the interaction between CO molecules adsorbed on metal particles. At $\theta_{CO} = 1$, the maximum of this band was observed at 2025 cm^{-1}, at low coverage $\theta_{CO} \approx 0$, the band was shifted towards low frequencies around 2000–2005 cm^{-1}. An additional band at 1900 cm^{-1} is seen on the 1FTCAT sample which is likely to be related to bridged carbonyls.

Adsorption of carbon monoxide under the same conditions on unmodified silica does not result in the appearance of any bands related to the adsorbed species.

DISCUSSION

The results obtained show the presence in the catalysts before reduction of at least two different Co species: Co_3O_4 crystalline particles and Co in an amorphous phase, which cannot be seen by XRD. The size of cobalt oxide crystallites and cobalt distribution between amorphous and crystalline phase can be controlled during the synthesis by using different alcohols. According to the literature, this amorphous phase can resemble amorphous cobalt silicate or can be amorphous silica with incorporated isolated Co^{n+} ions. The EXAFS data obtained for 5FTCAT which has a large concentration of Co amorphous phase (~88%) show the presence of Co atoms in the second and even third coordination sphere of cobalt. The CoO interatomic distances were found to be practically the same in the 5FTCAT sample and in Co_3O_4. Thus it can be suggested that the Co species in the 5FTCAT sample are likely to be small oxide clusters involving several Co atoms, probably small fragments of Co_3O_4 crystallites rather than isolated Co^{n+} ions as in the structure of cobalt silicate sometimes assumed in the literature.

FTIR experiments carried out with the 5FTCAT sample having a large concentration of Co amorphous phase showed that after calcination this sample contained low coordinated Co^{2+} or Co^{3+} ions. These unsaturated ions hardly reducible by hydrogen at the temperatures up to 873 K can be considered as an analogue of the Lewis acid sites which exist, for instance, in alumina or amorphous alumosilicates and may also as for aluminosilicates be involved in hydrocarbons reactions. It can be suggested therefore that these sites can considerably affect the activity and selectivity of the catalysts in the Fischer–Tropsch synthesis. Earlier Shriver and Sachtler (36, 37) showed that modification of Rh/SiO_2 catalysts with Lewis acids led to a considerable increase in the rate of CO insertion in the reaction of ethylene hydroformylation. Interaction of surface carbonyls with Lewis electron accepting sites was suggested to result in their higher reactivity.

The diameters of the Co_3O_4 particles evaluated from XRD data varied from 60 to 700 Å. As can be seen from the XRD and EXAFS data, this crystalline phase of Co_3O_4 supported by silica has different chemical properties than the crystalline bulk oxide. It can be decomposed to CoO and oxygen by heating at 623–673 K under nitrogen (Figs. 6, 7). The experiments carried out with bulk oxide did not show any decomposition of Co_3O_4 under nitrogen by heating to 873 K for 10 h.

The Co_3O_4 particles also have a different reducibility under hydrogen than the bulk oxide. As was shown, the reduction of Co_3O_4 with hydrogen proceeds in two steps: first, reduction of Co_3O_4 to CoO (473–573 K); then reduction (523–773 K) of CoO to Co metal. The Co reduction in the silica supported samples was followed by XRD, EXAFS, and FTIR. The temperature of reduction to CoO was about 473–523 K, whereas the temperature of reduction to metal was found to vary for the different samples. This observation is consistent with the earlier results of other authors (15, 16, 38). FTIR experiments carried out with the 5FTCAT sample with a large concentration of amorphous Co phase showed the absence of metal sites after the treatment of the sample at 723 K under hydrogen. It could therefore, be assumed that no reduction of the amorphous Co/silica phase occurred in the temperature range of 473–873 K.

As can be seen from Fig. 8, almost all Co_3O_4 crystallites can be reduced to the CoO phase. However, the CoO particles formed after the reduction of Co_3O_4 have different reducibility to metal species. The ease of reduction decreases with decrease in the particle size. Fig. 9 shows that the relative concentration of metallic cobalt was found to be higher for the samples with larger oxide particles, whereas on the samples with smaller oxide particles even after the reduction at 723 K a considerable concentration of CoO was observed. The same conclusions were drawn from *in situ* EXAFS experiments (Fig. 10). In the 4FTCAT sample Co oxidised species ($d_{Co_3O_4} = 200$ Å) can be reduced almost quantitatively to metal at 573–773 K, whereas in the 1FTCAT catalyst ($d_{Co_3O_4} = 60$ Å) even after treatment under hydrogen at 773 K only oxidised CoO species were detected.

The extent of Co_3O_4 reduction to the metal phase can be estimated in a more quantitative manner. The ratio of the intensity of the XRD peak (111) at $2\theta = 44.208^\circ$ attributed to the cubic metal phase measured for the reduced samples to the intensity of the XRD peak at $2\theta = 59.345^\circ$ (Co_3O_4(511)) measured for the oxidised sample could permit a comparison of the extent of reducibility of Co_3O_4 towards metal for the samples with different sizes of the Co_3O_4 crystallites (Fig. 13). As can be seen, the percentage of crystalline Co_3O_4 reduced to metal is clearly higher for the 4FTCAT and 5FTCAT samples than for the catalysts with small crystallite sizes (1FTCAT, 2FTCAT, 3FTCAT).

This result is in good agreement with the earlier data of Castner *et al*. (16) who studied hydrogen reduction properties of two Co catalysts supported on small and large pore silica. In that work it was found that the difficulty of the reduction step (CoO to metal) increases when decreasing the pore size of the silica and thus, cobalt oxide particle size.

The observed dependence of the reducibility of Co_3O_4 particles on their sizes in Co/SiO_2 catalysts cannot be explained in terms of kinetic or diffusion limitations during the reduction. In this case, larger particles should be more difficult to reduce. The more probable explanation lies in the effect of metal support interaction. It can be suggested that in smaller metal particles the interaction between metal and support is much stronger than in larger ones and this interaction is likely to stabilise small oxidised particles and clusters in silica. For instance, the 5FTCAT sample containing very small amorphous clusters of Co_3O_4 and the 1FTCAT sample with small crystalline particles (d = 60 Å) were the most difficult to reduce. Encapsulation of smaller Co particles by the silica matrix would make the reduction more difficult and might be one of the possible mechanisms of such interaction.

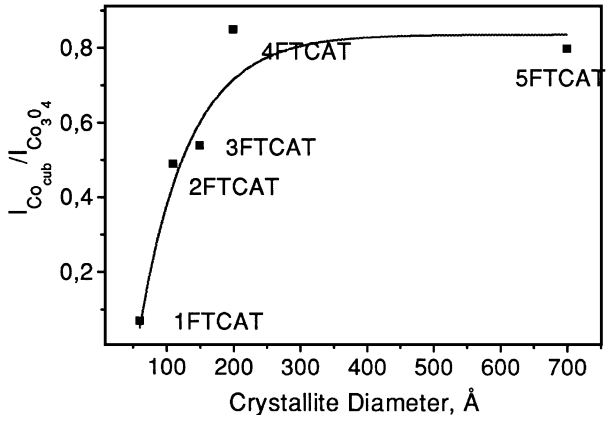

FIG. 13. Particle size dependence of the ratio of the intensity of the XRD peaks ($2\theta = 44.208^\circ$) attributed to cubic metal phase (111) in the samples after reduction to the intensity of Co_3O_4 (511) diffraction peaks ($2\theta = 59.345^\circ$) in the calcined samples.

The XRD data are in good agreement with the results of the FTIR experiments. As can be seen from Fig. 12, the highest intensity of the band at 2025 cm^{-1} which is related to CO molecules adsorbed on metal active sites in the catalysts was observed on the 4FTCAT sample. This catalyst contains prior to reduction most of the Co species in the form of crystalline oxide with a particle diameter of 200 Å. The intensity of the line at 2025 cm^{-1} and correspondingly, the concentration of active metal species was considerably lower on the other samples due either to a low concentration of the Co_3O_4 crystalline phase (5FTCAT) or to the relatively small size of the Co_3O_4 particles which are apparently difficult to reduce to metal phase with hydrogen at 723 K. In the samples with smaller particles (1FTCAT), a marked concentration of the bridged carbonyls ($\nu_{CO} = 1900$ cm^{-1}) was observed which probably can be assigned to higher concentrations of crystalline defects.

The intensity of the band at 2181 cm^{-1} was also found to vary between the samples. This band was most intense on the 5FTCAT samples which contains a high concentration of Co^{n+} ions in the amorphous phase.

The relative concentration of reduced Co and the metal surface sites, which are assumed to be involved in the Fischer–Tropsch synthesis, can be estimated both from XRD and FTIR results (intensity of the band at 2025 cm^{-1} in the spectra of adsorbed CO). The samples investigated in this study can be arranged in the following order characterising the decrease in the number of metal surface sites after the reduction at 723 K:

$$4FTCAT > 2FTCAT > 3FTCAT > 1FTCAT > 5FTCAT.$$

Analysis of the results gives evidence to suggest that to obtain a high concentration of metallic cobalt after reduction by hydrogen at 673–773 K cobalt should be present in the Co/SiO_2 catalysts after calcination in the form of relatively large crystalline Co_3O_4 particles. Thus, to produce a Co/silica catalyst with a maximal number of surface metal sites, an optimum between the crystallite size and reduction properties has to be achieved. Small particles have rather high surface area, but they are very difficult to reduce; larger

Co particles can be reduced much more easily, but their surface can be quite small.

Although it is difficult to correlate directly preparation conditions with the resulting distribution of cobalt between the observed phases, it can be seen that the presence of lower molecular weight alcohols during the catalysts synthesis leads to larger quantities of Co_3O_4 crystalline particles in the 100–200 Å size range and, thus, to higher overall reducibility of cobalt. Use of butanol in the preparation leads to rather large (700 Å) Co_3O_4 particles and to a higher concentration of amorphous phase, resulting in the lowest concentration of available metal sites in the reduced catalysts. Addition of formamide appears to result in a reduction of the size of Co_3O_4 particles leading to their lower reducibility.

CONCLUSIONS

A combination of techniques (*in situ* XRD, *in situ* EXAFS, and FTIR) providing information on local and long-range order allowed a clear picture of the phases present in Co/SiO_2 catalysts to be developed. Cobalt is present both as crystalline Co_3O_4 and in small (XRD amorphous) aggregates containing several Co atoms. Co in the amorphous phase was found to be not reducible under hydrogen up to 723 K.

The results obtained using *in situ* XRD, *in situ* EXAFS, and FTIR spectroscopy showed that the reducibility of Co_3O_4 crystallites supported on silica strongly depended on Co distribution between crystalline and amorphous phases and on the crystallites size. Heating of oxidised Co catalysts under inert atmosphere resulted in a selective transformation of Co_3O_4 to CoO crystalline particles at 623–673 K. The hydrogen reduction properties of particles of cobalt oxide to metal on silica were shown to depend on the size of crystallites. The ease of reduction decreased from larger (200–700 Å) to smaller particles (60 Å).

FTIR spectroscopy with CO as a molecular probe showed the presence of different active sites associated with Co after the reduction of the catalysts: Co metal sites, Co^{2+} ions in the crystalline phase of CoO and Co^{n+} ions in the amorphous phase.

ACKNOWLEDGMENT

The authors acknowledge the financial support of the European Union (Contract JOF3-CT95-0016).

REFERENCES

1. Anderson, R. B., "The Fischer–Tropsch Synthesis," Academic Press, New York, 1984.
2. Bond, G. C., "Catalysis by Metals," Academic Press, London/New York, 1962.
3. Haggin, J., *Chem. Eng. News*, **Oct. 26**, 24 (1981).
4. Haggin, J., *Chem. Eng. News*, **July 23**, 27 (1990).
5. Hindermann, J. P., Hutchings, G. J., and Kiennemann, A., *Catal. Rev. Sci. Eng.* **35**(1), 1 (1993).
6. Rathousky, J., Zukal, A., Lapidus, A., and Krylova, A., *Appl. Catal.* **79**, 167 (1991).
7. Roe, G. M., Ridd, M. J., Cavell, K. J., and Larkins, F. P., *Stud. Surf. Sci. Catal.* **36**, 509 (1988).
8. Arnoldy, P., and Moulijn, J. A., *J. Catal.* **93**, 38 (1985).
9. Colley, S. E., Copperthwaite, R. G., and Hutchings, G. J., *Catal. Today* **9**, 203 (1991).
10. Shirai, M., Inoue, T., Onishi, T., Asakura, K., and Iwasawa, Y., *J. Catal.* **145**, 159 (1994).
11. Asakura, K., Shirai, M., and Iwasawa, Y., *Catal. Lett.* **20**, 117 (1993).
12. Kazansky, V. B., Zaitsev, A. V., Borovkov, V. Yu., and Lapidus, A. L., *Appl. Catal.* **40**, 17 (1988).
13. Lapidus, A., Krylova, A., Kazanskii, V., Borovkov, V., Zaitsev, A., Rathousky, J., Zukal, A., and Jancalkova, M., *Appl. Catal.* **73**, 65 (1991).
14. Srinivisan, R., De Angelis, R. J., Reucroft, P. J., Dhere, A. G., and Bentley, J., *J. Catal.* **116**, 144 (1989).
15. Castner, D. G., Watson, Ph. R., and Chan, I. Y., *J. Phys. Chem.* **93**, 3188 (1989).
16. Castner, D. G., Watson, Ph. R., and Chan, I. Y., *J. Phys. Chem.* **94**, 819 (1990).
17. Castner, D. G., and Watson, Ph. R., *J. Phys. Chem.* **95**, 6617 (1991).
18. Haddad, J., and Goodwin, Jr., J. G., *J. Catal.* **157**, 25 (1995).
19. Lisitsyn, A. S., Golovin, A. V., Kuznetsov, V. L., and Yermakov, Yu. I., *J. Catal.* **95**, 527 (1985).
20. Reuel, R. C., and Bartholomew, C. H., *J. Catal.* **85**, 78 (1984).
21. Shao, Y., Chen, W., Wold, E., and Paul, J., *Langmuir* **10**, 178 (1994).
22. Reuel, R. C., and Bartholomew, C. H., *J. Catal.* **85**, 63 (1984).
23. Rao, U. S., and Gormley, R. J., *Hydrocarbon Process.* **59**, 139 (1980).
24. Dhere, A. G., De Angelis, R. J., and Reucroft, P. J., *J. Mol. Catal.* **20**, 301 (1983).
25. Davydov, A. A., "IR Spectroscopy of Adsorbed Species on the Surface of Transition Metal Oxides," Wiley, New York, 1991.
26. Heal, M. J., Leisegang, E. C., and Torrington, R. G., *J. Catal.* **51**, 314 (1978).
27. Choi, J.-G., Rhee, H.-K., and Moon, S. H., *Appl. Catal.* **13**, 269 (1985).
28. Sinfelt, J. H., Via, G. H., and Lytle, F. M., *Catal. Rev. Sci. Eng.* **26**, 81 (1984).
29. Bart, J. C., and Vlaic, G., *Adv. Catal.* **35**, 1 (1989).
30. Short, D. R., Mansour, A. N., Cook, J. M., Sayers, D. E., and Katzer, J. R., *J. Catal.* **82**, 299 (1983).
31. Michalowicz, A., "Méthodes et Programmes d'Analyse des Spectres d'Absorption des Rayons X," Ph.D. thesis, Université Paris, Val de Marne, 1990.
32. Huffmann, G. P., Shah, N., Zhao, J., Huggins, F. E., Hoost, T. E., Halvorsen, S., and Goodwin, J., *J. Catal.* **151**, 17 (1995).
33. Rehr, J. J., Zabinsky, S. I., and Albers, R. C., *Phys. Rev. Lett.* **69**, 339 (1992); Rehr, J. J., *J. Appl. Phys.* **32**, 8 (1993); Rehr, J. J., Mustre de Leon, L., Zabinsky, S. I., and Albers, R. C., *J. Am. Chem. Soc.* **113**, 5135 (1991); Mustre de Leon, J., Rehr, J. J., Zabinsky, S. I., and Albers, R. C., *Phys. Rev. B* **44**, 4146 (1991).
34. Canesan, P., Kuo, H. K., Saavedra, A., and De Angelis, R. J., *J. Catal.* **52**, 310 (1978).
35. Nyquist, R. A., and Kagel, R. O., "IR Spectra of Inorganic Compounds," Academic Press, New York, 1971.
36. Richmond, T. G., Basolo, F., and Shriver, D. F., *Inorg. Chem.* **21**, 1272 (1982).
37. Ichikawa, M., Lang, A. J., Shriver, D. F., and Sachtler, W. M. H., *J. Am. Chem. Soc.* **107**, 7216 (1985).
38. van't Blik, H. F., and Prins, R., *J. Catal.* **97**, 188 (1986).